Nanometer Localization of Single Green Fluorescent Proteins: Evidence that Myosin V Walks Hand-Over-Hand via Telemark Configuration

Gregory E. Snyder,* Takeshi Sakamoto,‡ John A. Hammer, III,§ James R. Sellers,‡ and Paul R. Selvin*†
*Physics Department and †Center for Biophysics and Computational Biology, University of Illinois Urbana-Champaign, Urbana, Illinois; and ‡Laboratory of Molecular Cardiology and §Laboratory of Cell Biology, National Heart, Lung and Blood Institute, National Institutes of Health, Bethesda, Maryland

ABSTRACT Myosin V is a homodimeric motor protein involved in trafficking of vesicles in the cell. It walks bipedally along actin filaments, moving cargo ~37 nm per step. We have measured the step size of individual myosin heads by fusing an enhanced green fluorescent protein (eGFP) to the N-terminus of one head of the myosin dimer and following the motion with nanometer precision and subsecond resolution. We find the average step size to be 74.1 nm with 9.4 nm (SD) and 0.3 nm (SE). Our measurements demonstrate nanometer localization of single eGFPs, confirm the hand-over-hand model of myosin V procession, and when combined with previous data, suggest that there is a kink in the leading lever arm in the waiting state of myosin V. This kink, or "telemark skier" configuration, may cause strain, which, when released, leads to the powerstroke of myosin, throwing the rear head forward and leading to unidirectional motion.

INTRODUCTION

Myosin V is a processive motor involved in transporting vesicles and organelles in the cell (Mehta, 2001). It contains two "heads" held together by a coiled-coiled cargo-carrying stalk. Each head contains a globular domain responsible for actin binding and ATP hydrolysis, and an ~24-nm-long α-helix bound to six calmodulins that likely act as a lever arm to amplify small nucleotide-dependent conformational changes in the globular domain (Forkey et al., 2003; Howard, 1997; Mehta, 2001; Purcell et al., 2002). The cargo, or center of mass, moves 35–40 nm for each ATP hydrolyzed (Ali et al., 2002; Forkey et al., 2003; Mehta et al., 1999; Rief et al., 2000; Rock et al., 2001). Recent work has shown that myosin V moves processively along actin in a "hand-over-hand" or "walking" manner in which each head takes turn in the lead (Forkey et al., 2003; Yildiz et al., 2003). The rear head translates 74 nm, moving past the front head, which remains stationary, and the cargo is moved ~37 nm for each step (Fig. 1). This is in contrast to an inchworm model, which has, for example, been postulated for kinesin (Hua et al., 2002). In an inchworm model, all parts of the motor protein translate uniformly—for myosin V, this would be 37 nm.

How the two heads are coordinated in the hand-over-hand mechanism is a central unresolved question. Nucleotide-hydrolysis, actin-binding, and lever arm position are likely tightly coupled (Veigel et al., 2002). Unidirectional motion implies functional asymmetry between the heads to create out-of-phase binding and hydrolysis. For example, to create a forward step, the front head should be tightly bound whereas the rear head is not bound. One model postulates that ATP binding to the rear head releases that head, which is then thrown forward by strain created previously in the myosin (Rief et al., 2000; Spudich, 2001). (To prevent binding of ATP and release of the front head, strain-induced inhibition of ATP binding to the front head has been postulated in the kinesin motor (Rosenfeld et al., 2003).)

The location of this strain is uncertain. An attractive model is the "telemark skier," where the front head is bent or kinked (Fig. 1, *right*) (Burgess et al., 2002; Spudich, 2001; Walker et al., 2000). When the rear head binds ATP and is released from actin, the strain released from the bend would tend to throw the rear head forward. A sharp bend in the front head was seen in some negatively stained myosin V images, where the bend was interpreted to be just before the lever arm—most likely in the pliant region (Dominguez et al., 1998) between the converter domain (part of the catalytic domain) and the first IQ motif of the lever arm (Walker et al., 2000). More gentle distortions in the lever arm itself were also observed, and other myosin Vs appeared to have straight lever arms. The subset of lever arms that fell into a relatively straight configuration were analyzed in detail in a later article that showed that the rear head was in a postpowerstroke conformation and the leading head was in a prepowerstroke conformation (Burgess et al., 2002).

An alternative telemark skier model places the bend directly in the lever arm. This model makes two testable predictions. First, as noted by Forkey et al., a dye rigidly attached to a calmodulin below the kink will not reorient during a step, whereas a dye placed above the kink will reorient (Forkey et al., 2003). Forkey et al. observed two populations of dyes, one that rotated, and one that did not rotate during a step, although the locations of the dyes corresponding to these two populations were not determined (Forkey et al., 2003). Second, the step size of a dye below the

Submitted November 5, 2003, and accepted for publication May 18, 2004.

Address reprint requests to Paul R. Selvin, Loomis Lab of Physics, 1110 W. Green St., University of Illinois Urbana-Champaign, Urbana, IL 61801. Tel.: 217-244-3371; Fax: 217-244-7559; E-mail: selvin@uiuc.edu.

0006-3495/04/09/1776/08 $2.00

doi: 10.1529/biophysj.103.036897

kink will alternate between 74 nm and 0 nm—the same as a dye on the globular domain—whereas the step size of a dye above the kink will alternate between a large step that is <74 nm, and a small step that is >0 nm (Fig. 1). Finally, a telemark skier configuration in which the bend is in the converter domain below the lever arm, such as that suggested by Walker et al. (2000), leads to stepping of <74 nm and >0 nm for a dye anywhere in the lever arm, i.e., a stepping pattern characteristic of a straight lever arm.

Yildiz et al. (2003) developed a technique where the position of a dye could be located with 1.5 nm precision, with subsecond temporal resolution (fluorescence imaging one nanometer accuracy (FIONA)). Using FIONA, they measured step sizes and showed that a dye on a calmodulin could step 74 and 0 nm. Assuming the catalytic domains are 37 nm apart, i.e., take 74 nm steps, this result suggests a ''telemark skier'' configuration in which the lever arm is bent. However, because labeling on the globular domain was not done by Yildiz et al. (2003), a direct measurement of the globular domain step size is necessary to confirm the telemark model with a lever arm bend.

We now extend FIONA to enable nanometer localization of single GFPs and measure the step size of the globular domain of myosin V. Others have previously imaged single GFPs bound to kinesin (Pierce et al., 1997), and 30 nm localization with 5 ms temporal resolution (Kubitscheck et al., 2000; Schmidt et al., 1996) has been achieved. Here we have constructed a heterodimeric myosin V containing an N-terminal eGFP on one catalytic domain, with the other head unlabeled. We show 4–10 nm localization of single GFP with subsecond temporal resolution and a photostability that enables typical observation times of ~25 s, with observation times as long as 75 s. Control experiments using a nanometric stage verify our ability to accurately measure step sizes. ATP-induced myosin V steps are also measured. We find the globular domain takes 74 nm steps, which, when combined with the results of Yildiz et al. (2003) supports a telemark skier model with a bend in the front lever arm.

MATERIALS AND METHODS

Total internal reflection fluorescence microscopy

Total internal reflection fluorescence (TIRF) microscopy was used to excite and image single eGFPs on myosin V, or eGFPs placed directly on a coverslip for control experiments. A similar TIRF microscope has been described (Yildiz et al., 2003). The image of a single dye, called the point-spread function (PSF) has a width of $\sim\lambda/2$, or ~250 nm for visible excitation. However, the center of the PSF, which, under appropriate conditions, represents the position of the dye (Bartko and Dickson, 1999a,b), can be determined with nanometer precision (Thompson et al., 2002; Yildiz et al., 2003). We use a two-dimensional (2-D) Gaussian fit to the PSF, described further below.

Experiments were performed using objective-type TIRF (Tokunaga et al., 1997) on an Olympus IX-70 microscope. Stage-stepping experiments in which a GFP was immobilized on a coverslip and the coverslip translated in 36 nm steps were performed with an Olympus 60× 1.45 numerical aperture (NA) oil immersion objective, magnified by a 1.5× microscope lens. Myosin motility experiments were done with an Olympus 100× 1.65 NA objective, and rarely with the 1.45 NA objective. Samples were illuminated with the 488 nm line of an Ar-ion laser (model 543-AP-A01, Melles Griot, Carlsbad, CA). The laser power was ~0.5 mW entering the microscope with the 100× objective and a spot size of ~12 μm in diameter, and ~2 mW with the 60× objective and a spot size of ~18 μm. A Q505LP dichroic and HQ550/100 emission filter (Chroma, Rockingham, VT) were used to separate excitation from fluorescence. Images were collected with a scientific

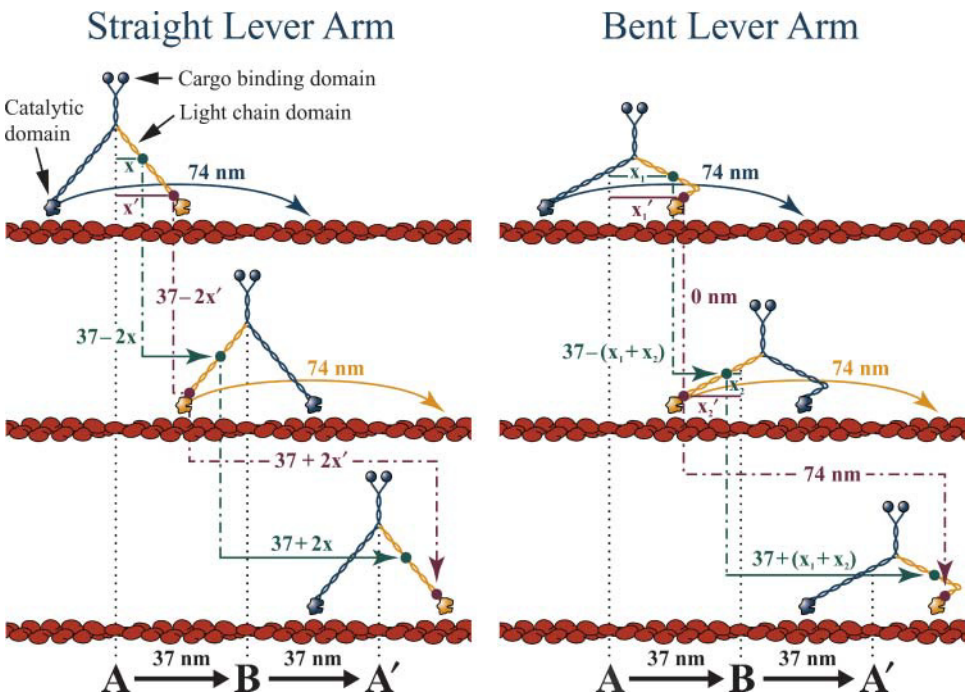

FIGURE 1 Schematic of hand-over-hand model of myosin V processitivity when the leading myosin V lever arm is straight (*left*) or has a bend (*right*). The step size of a dye (*green* or *purple dots*) alternates between small and large: $\{37 - (x_1 + x_2)\}$, followed by $\{37 + (x_1 + x_2)\}$, where x_1 and x_2 are the distances from the midpoint between the globular domains along the direction of motion, before and after the step, respectively. With a straight lever arm, $x_1 = x_2 \equiv x$, and the step sizes are larger and smaller than 0 nm and 74 nm, respectively ($2x' < 37$ nm), for a dye anywhere on the lever arm. In the bent-lever-arm model, the same stepping pattern is seen for a dye above the bend: however, a dye below the bend (*purple dot*) takes alternating 0 nm, 74 nm steps ($x_1' + x_2' = 37$ nm). In either model, the catalytic domain step size, as measured by a GFP attached to the N-terminus, is 74 nm.

grade, back-thinned, frame transfer charge-coupled device camera (Micromax 512BFT, Roper Scientific, Trenton, NJ), consisting of a 512 × 512 array of 13 μm × 13 μm pixels. The camera can acquire a full frame in 0.35 s without any significant dead time at 1 MHz readout rate. Background noise in the camera is limited by readout noise: 0.5 counts/pixel/s comes from dark current and 5.9 counts/pixel/s from readout noise. All experiments were performed by integrating 0.5 s/frame.

Sample chamber preparation

Microscope slides were prepared before cleaning by drilling two holes separated by 1–1.5 cm with a 3/4 mm diamond drill bit (see Supplementary Material). The holes become the entrance and exit holes for solutions to be flowed through the chamber. Sample chambers were prepared by sonicating microscope coverslips and slides separately for 30 min in acetone, followed by a thorough rinse and sonication with doubly deionized water, then 30 min sonication in 1 M KOH, and then rinsed and sonicated for 15 min in doubly deionized water. A sample chamber was assembled from a clean coverslip and microscope slide by placing double-sided tape next to the holes and placing a clean coverslip over the tape. The ends were sealed with epoxy. The volume of the chamber is 10–20 μL. For the myosin motility studies, photobleaching of any fluorescent contamination after a few minutes during the long (~1 h) observation times further reduced background. These extended observations in a single field were possible because the myosin continually comes out of solution, and then walks along actin. Fluorescent myosin could easily be distinguished from fluorescent dirt by its ability to move.

Stage-stepping experiment

eGFP (Clonetech, Palo Alto, CA) was immobilized onto a streptavidin-coated coverslip as follows. eGFP was biotinylated by reacting with a 20-fold excess of sulfo-NHS-biotin (Pierce, Rockford, IL) for 3.5 h in phosphate-buffered saline (PBS). Unreacted biotin was removed by dialyzing twice for 4 h in PBS using 10,000 Da cutoff dialysis bags. The flow cell was treated with 50 μL 1 mg/ml BSA-biotin (Sigma, St. Louis, MO) in T50 (10 mM Tris pH 8.0, 50 mM NaCl), and 50 μL 0.2 mg/ml streptavidin (Molecular Probes, Eugene, OR), allowed to react 10 min, and then washed with T50. Biotinylated-eGFP (25–250 pM) was then added in T50, and excess sometimes washed with T50. The coverslip was translated (NanoH-70 stage, 0.7 nm position accuracy in closed-loop mode, MadCity Labs, Madison, WI) in 36 nm steps. The step size was determined by a calibrated stage and verified by imaging very bright fluorescent beads in which we find an average of 35.4 nm ± 0.2 nm (mean ± SE).

eGFP-myosin V preparation and in vitro motility assay

Production of recombinant baculoviruses driving the expression of heavy meromyosin-like (HMM) fragments of the mouse myosin V were produced as described by Wang et al. (2000). Addition of eGFP at the amino-terminus of the heavy chain was performed as described in Wu et al. (2002). This fusion introduced two alanine residues between the C-terminus of GFP and residue 2 of the myosin V heavy chain. Infection of Sf9 cells and purification of eGFP-labeled myosin V HMM were as described (Wang et al., 2000). Singly labeled eGFP-myosin V was prepared via infection in SF9 cells with a 1:10 ratio of virus for eGFP-myoV and unlabeled myoV along with a virus driving the expression of calmodulin. The resulting preparation was run on an SDS gel, and that the ratio of GFP-HMM/HMM was found to be 0.27. If the two heavy chains recombined randomly then one would expect a binomial distribution of GFP-HMM/HMM, resulting in 7% GFP-HMM homodimers, 53% HMM homodimers, and 39% GFP-HMM/HMM heterodimers. The expected fraction of the total fluorescent spots resulting from homodimers is therefore $7/(39 + 7) \times 100\% = 15\%$.

Myosin V with eGFP on both heads was also made and an in vitro motility assay was performed at 37°C, as described previously (Sakamoto et al., 2003). (Buffer conditions were: 50 mM KCl, 20 mM MOPS pH 7.4, 5 mM $MgCl_2$, 0.1 mM EGTA, 2 mM ATP, 50 mM DTT, with the oxygen scavenger system of Harada et al. (1990).

Motility assay

Actin filaments were immobilized on a coverslip and myosin V was allowed to move on actin in the presence of ATP. The protocol closely follows published procedures (Forkey et al., 2003; Yildiz et al., 2003) except nitrocellulose was not used, and bovine serum albumin (BSA) was added to the solution. A deoxygenation system was not used. Briefly, the sample chamber was prepared by flowing 10 μM BSA-biotin, waiting for 2 min, washing with M5BufBH (20 mM HEPES pH 7.6, 2 mM $MgCl_2$, 25 mM KCl, 1 mM EGTA) plus 10 mM DTT and 100 μg/ml calmodulin (M5+), followed by 0.5 μg/ml streptavidin, waiting for 2 min, followed by 0.2 μM 1:10 biotinylated/unbiotinylated phalloidin-stabilized F-actin, followed by M5+ wash, followed by myosin V sample solution. Myosin V sample solution consists of 0.3–1.8 nM eGFP-myosin V, 2.5 mg/ml BSA, 100 mM DTT, 100 μg/ml calmodulin, and 2–4 μM ATP, in M5BufBH. A deoxygenation system was not used because previous work (Swaminathan et al., 1997), as well as our own limited data, indicate no significant photostability enhancement of eGFP upon deoxygenation.

Data acquisition and analysis

Data acquisition and analysis has been described (Yildiz et al., 2003). Briefly, images are captured using the MicroMax camera (Roper Scientific, Tucson, AZ) and saved as multiimage TIF files. A laboratory written program in IDL (Research Systems, Boulder, CO) is used to fit a PSF in successive frames to a 2-D Gaussian function. The position of the center is then used to calculate the step size using scripts written in Octave (www.octave.org), with appropriate statistical weighting according to the uncertainty in position before and after a step (Yildiz et al., 2003). Individual PSFs are fit and analyzed in Sigma Plot (SPSS, Chicago, IL).

Theoretical considerations on localization limits

The relation between the SE (σ_μ), i.e., the uncertainty in the center, and the number of collected photons (N), the effective pixel size of the imaging detector (a), the standard deviation of the background (b), which includes noise due to background fluorescence and the detector, and the width of the distribution (SD, σ_i, in direction i) was derived by Thompson et al. (2002) in two dimensions:

$$\sigma_{\mu_i} = \sqrt{\left(\frac{\sigma_i^2}{N} + \frac{a^2/12}{N} + \frac{8\pi\sigma_i^4 b^2}{a^2 N^2}\right)}, \quad (1)$$

where the index i refers to the x- or y-direction. The first term (σ_i^2/N) is the photon noise, the second term is the effect of finite pixel size of the detector, and the last term is the effect of background. For our experiments, the camera pixel size is 13 μm, corresponding to a = 144.3 nm with 90× magnification, or 130 nm with 100× magnification; b is typically 10–14 photons (variance of camera dark-counts and background fluorescence is 9 and 4.4–9.4, respectively).

RESULTS AND DISCUSSION

Control experiments

To demonstrate our ability to precisely locate the position of individual eGFPs, the fluorescent proteins were biotinylated

and immobilized on a coverslip. A diffraction-limited image of a single eGFP with 0.5 s integration time, with a 2-D Gaussian fit (*solid lines*) overlaid, is shown in the top left inset of Fig. 2. The uncertainty in the PSF center is <4 nm: $\sigma_{\mu_x} = 3.3$ nm; $\sigma_{\mu_y} = 3.9$ nm. The sample was then translated using a nanometric stage in uniform 36 nm (based on stage voltage) step sizes, one step every 3 s. The 36 nm step size was verified by imaging very bright, unpolarized fluorescent beads and measuring the distance between the PSF centers before and after each step, where we found 35.4 ± 0.2 nm. Fig. 2 shows the PSF center position of each 0.5 s eGFP image versus time. Steps are clearly discernable. The average of the four steps is 34.7 ± 4.1 nm (σ), in good agreement with the expected value. The average of 25 steps taken from several eGFPs is 36.2 nm ± 4.3 nm (σ).

To test the functionality of the eGFP-myosin V, a myosin V with an eGFP on both heads was constructed and its in vitro motility was compared to wild type at saturating [ATP]. The results are: 358 ± 42 nm/s, compared to wild type of 380 ± 90 nm/s, indicating nearly wild-type activity for the eGFP-myosin.

Measuring eGFP-myosin V steps

Fig. 3 shows the PSF of an eGFP-myosin V bound to an immobilized actin filament and fit to a 2-D Gaussian (*solid black lines*). One-thousand six-hundred and twenty-six photons were collected in 0.5 s. The width (σ) is ± 146 nm, corresponding to a full-width-half-maximum of 321 nm; the uncertainty in the center position (σ_μ) is 6.9 nm.

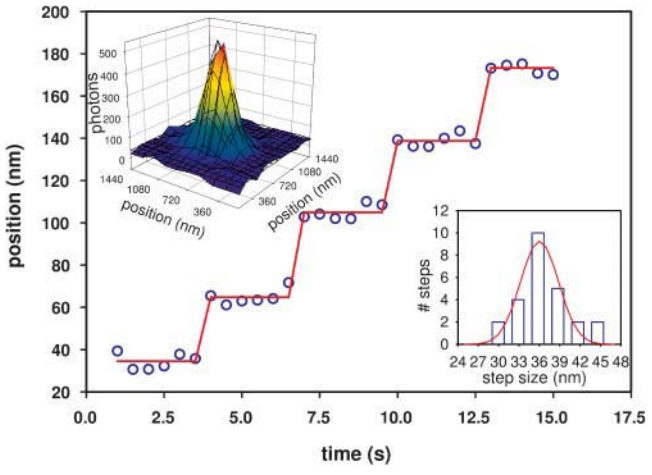

FIGURE 2 Point-spread function (*top left inset*) and stage-stepping data of eGFP with histogram (*bottom right inset*) immobilized on coverslip. For the PSF shown, $\sigma_{\mu x} = 3.3$ nm, $\sigma_{\mu x} = 3.9$ nm. The stage was moved uniformly an average of 35.7 nm ($\sigma_\mu = 0.18$ nm; $\sigma = 0.45$ nm; $N_{steps} = 7$) once every 3 s. Open blue circle is the position of the dye based on Gaussian fitting of the PSF in each 0.5 s image. The red line is the average position of the dye based on averaging the open blue circles. The average step size for this molecule is measured to be 34.7 ± 4.1 nm (mean ± SD). The average of 25 steps (*bottom right inset*) is 36.2 nm ± 4.3 nm.

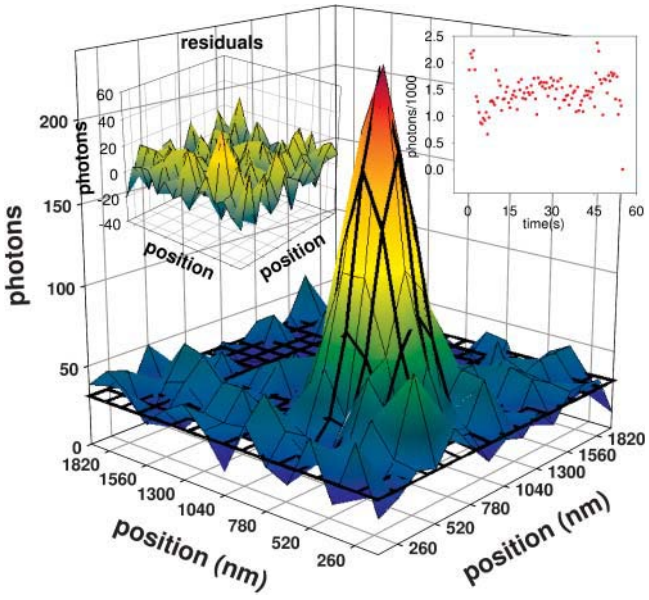

FIGURE 3 Point-spread function of eGFP on myosin V, fit to a 2-D Gaussian (*solid black lines*). A total of 1626 photons were collected in 0.5 s. The peak pixel contained 240 photons; σ_x (width in *x*-direction) = 146 nm; σ_y (width in *y*-direction) = 147 nm; $\sigma_\mu = 6.9$ nm. The fit is excellent: $\chi^2 = 0.99$ and residuals (*left inset*) show no structure. This molecule lasted 55 s (*right inset*), with an average of 1444 ± 298 photons collected photons per 0.5 s image.

According to Eq. 1 (with $b = 8.3$ and $a = 130$ nm), σ_μ. is expected to be 5.6 nm, somewhat smaller than the 6.9 nm found by curve fitting. The difference is likely due to approximations in the theoretical derivation, which Thompson et al. (2002) found tend to lead to 30% underestimation of the actual σ_μ values. The residuals display no systematic structure and $\chi^2 = 0.99$, indicating a Gaussian is an excellent approximation to the PSF shape. This is particularly important because finite emission polarization can lead to PSFs that deviate significantly from a Gaussian, particularly in the presence of spherical aberrations (Bartko and Dickson, 1999a,b). Under such conditions, the center of the PSF does not necessarily correspond to the position of the dye. An intensity-versus-time trace is shown in the right-hand inset. The average number of collected photons per 0.5 s image is 1444. The standard deviation is 298, which is significantly larger than 38 ($\sqrt{1444}$), the expected standard deviation if the eGFP was a simple Poisson emitter. This implies that the eGFP is likely blinking on and off at variable rates during the acquisition time (Peterman et al., 1999). This blinking, however, has no effect on the PSF shape; it simply causes the overall intensity to fluctuate, and hence σ_μ to vary from image to image.

Fig. 4 shows movement of eGFP-myosin V in the presence of 1–2 μM ATP, and Fig. 5 displays a histogram of step sizes. Two peaks are clearly visible in Fig. 5. Molecules are classified as small steppers if their step size is smaller than the cusp at 52 nm between the two peaks and large steppers if

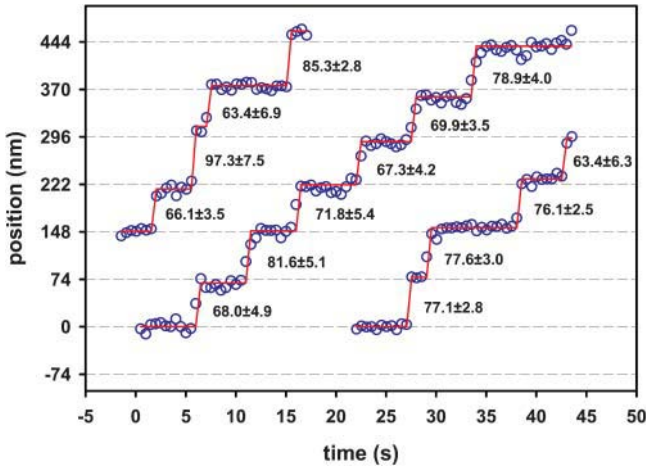

FIGURE 4 ATP-induced stepping of eGFP-myosin V for three different myosin Vs. The zero-time point is arbitrary. The horizontal red lines are the fit to the average position between each step. The values are average step size plus mean ± SE. [ATP] ≈ 1–2 μM.

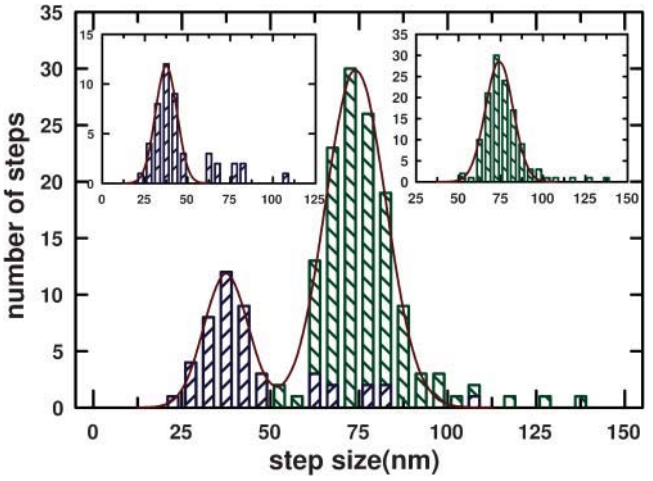

FIGURE 5 Histograms of eGFP-myosin V step sizes (*bars*) and curve fits (*lines*). The main figure contains all of the measured steps, and represents the composite of the two histograms in the insets. The left inset is a histogram of small/mixed steppers, and the right inset is the histogram of large steppers. The contributions of the inset histograms to the main histogram are represented by their respective colors and crosshatching. The composite histogram is fit to a sum of two Gaussians, yielding the same fit parameters for each peak as the fits to the individual peaks in the insets. The large peak has a mean of 74.1 nm with $\sigma = 9.3$ nm, $\sigma_\mu = 0.33$ nm. The Gaussian fit yields a mean of 74.1 nm, $\sigma = 8.5$ nm. The small peak has a mean of 35.9 nm with $\sigma = 6.3$ nm, $\sigma_\mu = 0.5$ nm. The Gaussian fit has a mean of 37.5 nm, with $\sigma = 6.2$ nm. The composite histogram contains 172 steps from 60 myosin V molecules. The histogram of small/mixed steppers contains 47 steps from 11 myosin V molecules. The minimum, maximum, and mean observation time before sudden loss of fluorescence due to photobleaching or myosin V diffusing away from surface is 4.5, 75, and 25 s, respectively.

their step size is larger than the cusp. Mixed steppers exhibit a mixture of small and large step sizes.

The distribution of large steppers is centered around 74.1 nm. This is consistent with a hand-over-hand model of myosin V motility in which the rear head moves twice the 37 nm stalk distance, and the front head does not move. The 0 nm steps taken by the labeled head when the unlabeled head moves are not observed directly. The 74 nm steps are not consistent with an inchworm model, where all parts of the myosin move a uniform 37 nm. This result, therefore, provides confirmation of the hand-over-hand model, consistent with that found by Yildiz et al. (2003).

We interpret the minor peak centered at 37.5 nm as arising from myosin Vs with eGFP on both heads. (The two eGFPs are sufficiently close that they cannot be resolved into two separate PSFs.) With one eGFP moving 74 nm and the other stationary, the apparent average movement is 37 nm. One molecule, for example, took nine uniform steps of average size 37.4 ± 2.1 nm (σ) before suddenly disappearing by photobleaching or detatching from actin. Because it photobleached in a single step, we cannot unambiguously conclude that it had two eGFPs. However, it emitted 460,000 photons, roughly twice the intensity we usually see for single eGFPs.

Arguments that other small and mixed steppers were eGFP-HMM homodimers follow:

1. Fig. 6 compares the intensity of eGFP-myosin Vs to the pattern of steps taken by each molecule. Fig. 6 *A* shows that 60% of small steppers were brighter than 98% of large steppers, consistent with small steppers being eGFP-HMM homodimers. The mixed steppers are not clearly distinguishable from large or small steppers in this figure, as may be expected if the mixed step sizes result from homodimers where one eGFP bleaches or blinks. A pattern of sequential bleaching followed by an increase in step size was not observed with mixed steppers, but all (save one) of them showed an intensity variation of a factor of two over their lifetimes.
2. Fig. 6 *B* shows the standard deviations of each molecule's intensity fluctuations normalized by the expected Poisson noise versus the pattern of steps taken. Normalizing by the expected Poisson noise reveals fluctuations not due to photon statistics, such as fluctuations caused by blinking, changes in the number of fluorophores in an observation spot, and reorientation of the fluorophore in the polarized excitation field. If all of the observed fluctuations in intensity result from Poisson noise, the ratio should be unity. If the fluctuations do not arise from Poisson noise, then the more fluctuating molecules present in an observation volume (here, a PSF), the smaller the amplitude of the fluctuations will be. Fig. 6 *B* shows that small steppers exhibit smaller fluctuations than large steppers, as would be expected if large steppers are heterodimers and small steppers are homodimers. Once again, the mixed steppers show a greater spread in their behavior, as expected if the mixed steps result from changes in the number of eGFPs being observed because of blinking or bleaching.

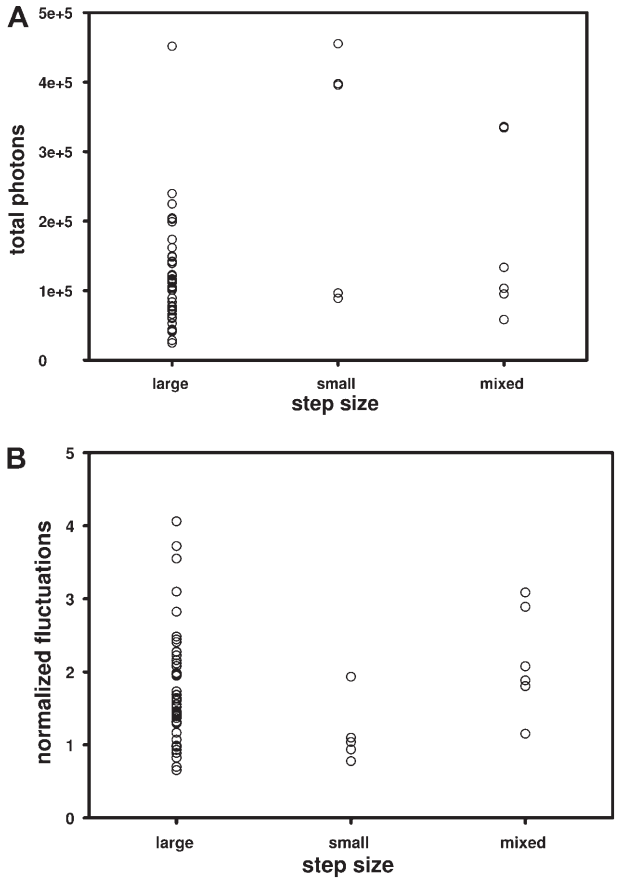

FIGURE 6 Analysis of the intensities of eGFP-myosin V demonstrates differences between molecules with different patterns of step sizes. (*A*) The total number of photons emitted by each eGFP-myosin V versus step size. The heterogeneity in eGFP brightness is clearly visible. Small steppers are nearly twice as bright as large steppers, arguing that two eGFPs are present in the spot. (*B*) Standard deviation of the number of photons per frame normalized by Poisson noise and plotted versus stepping pattern. Small steppers exhibit smaller fluctuations than large steppers, as expected for homodimers. See discussion in text.

3. The percentage of small/mixed steppers is $11/60 \times 100\% = 18\%$, consistent with the percentage of homodimers expected from the ratio of eGFP-HMM/HMM measured (15%; cf. Materials and Methods).
4. No 37-nm steps were observed in previous experiments (Yildiz et al., 2003).

Finally, the stepping rate of eGFP-myosinV was somewhat slower than expected based on the presumed 1–2 μM [ATP]. For example, the average rate in Fig. 4 is 0.18 s^{-1}, similar to that seen for exogeneously labeled myosin V at ~0.3 μM [ATP] (Yildiz et al., 2003). The cause of this is not known, although the actual [ATP] may differ from the expected value because of dead volume associated with buffer exchange.

GFP-FIONA

These measurements show that we can achieve ≥3 nm localization with eGFP. Previously, ~1 nm localization was achieved with exogenous dyes. Although the FIONA technique in each case is fundamentally the same, there are some detailed differences. In general eGFP is less bright and photostable than optimized single-molecule dyes such as Cy3, rhodamine, etc. Blinking with eGFP (and rhodamine dyes; Yildiz et al., 2003) with 0.5 s images was present but did not significantly impede nanometer localization. We found the 1.65 NA objective lens was advantageous compared to the 1.45 NA lens with eGFP. (The 1.65 NA objective was not tested with exogenous dyes.) Roughly 1.5 times higher signal/background was achieved with the 1.65 NA objective. This improvement likely comes from a combination of different sources: A), the higher numerical aperture is expected to collect 1.3 times more fluorescent photons; B), we found that background fluorescence from the specialized (Olympus, Tokyo, Japan) coverslips used with the 1.65 NA was ~2× lower than the conventional coverslips used with the 1.45 NA objective. (Autofluorescence from the oil was significantly less than from the coverslip.); and C), the higher index of refraction of the 1.65 NA coverslips means the intensity of the evanescent electric field is ~7 times higher than the electric field in the coverslip, at the critical angle, compared with a factor of 5 for the 1.45 NA lens (Axelrod, 1989), which again leads to higher signal/background.

Position and nature of the bend

Here we find that an eGFP on the catalytic domain takes 74 nm steps, and previously Yildiz et al. (2003) found a dye on an exchanged calmodulin also takes 74 nm steps. A trivial reason explaining how both step sizes can be the same, is that the labeled calmodulin is bound to the catalytic domain. However, we think this unlikely because there is no evidence that the catalytic domain of myosin V has such a binding site. In contrast, the lever arm (light-chain domain) contains six IQ domains, capable of binding calmodulin. We, therefore, assume that the calmodulin-labeled dye is indeed on the lever arm.

For both the catalytic domains and a dye on the lever arm to take the same alternating 74 nm and 0 nm steps, both the catalytic domains and the dye positions must be 37 nm apart from the midpoint between the two heads (Fig. 1). This implies that the lower part of the front and rear lever arms, where the dye is located, are parallel. This is not consistent with both lever arms being straight (Fig. 1, *left*), and implies a bend in one or both lever arms. Fig. 1 (*right*) shows one scenario where all of the bend is in the forward lever arm. It is theoretically possible that the bend/curvature is uniformly distributed between the front and rear lever arms. However, a bend in the front lever arm is functionally more advantageous because all the strain in this lever arm, when released, would go into moving the rear head forward, whereas a bend in the rear lever arm would not. Furthermore, Walker et al. (2000) and Burgess et al. (2002) concluded from electron

microscopy images of myosin V that the rear head is in the postpowerstroke state. This would tend to angle the rear lever arm forward, in a relatively straight position, as depicted in Fig. 1 (*right*). If the lever arms are indeed parallel and the rear head is in the postpowerstroke position, this implies that the front head also has the lever arm in the postpowerstroke position. This would appear to be at odds with the conclusion of Walker et al. (2000) and Burgess et al. (2002).They fit electron microscopic images of the front head into the x-ray structures of the pre- and postpowerstroke states that differ by ~5 nm in the position where the lever arm emerges from the motor domain, which should correspond to the position of the converter domain; they concluded that the front head was in the prepowerstroke state. A 5 nm movement of the converter domain, would likely lead to an ~8 nm movement of a dye near the bottom of the lever arm. This would lead to dye step sizes for a dye that alternates between 8 nm and 66 nm. Given the 1–4 nm localization precision in Yildiz et al. (2003), this is clearly different from the alternating 0 nm and 74 nm found.

Simple geometric arguments indicate that the kink must be fairly close to the catalytic domain, most likely between the first and second calmodulins. The lever arm is ~24 nm in length (Howard, 1997), or 4 nm/calmodulin, and the distance between catalytic domains is 37 nm; see Fig. 1, drawn to scale. (Thirty-seven nanometers corresponds to 13 actin monomers apart. The domains can also bind 11 or 15 monomers apart; Burgess et al., 2002; Walker et al., 2000; Yildiz et al., 2003). If the kink is between the first and second calmodulins, then the remaining 10 calmodulins can span 40 nm, enough to span the distance if extended. A kink between the second and third calmodulins leaves only eight calmodulins to span 37 nm, which is unlikely.

SUMMARY

The 74 nm steps observed with individual eGFP-myosin V are further support of a hand-over-hand model for myosin V, consistent with our earlier studies using exogenous fluorophores placed on the light-chain domain of myosin V (Yildiz et al., 2003). In addition, the 74.3 nm steps of the GFP on the globular domain are essentially identical to the 73.8 nm found previously for a dye on the light-chain domain, 18.5 nm from the midpoint along the direction of motion (Yildiz et al., 2003). This in turn implies there is a kink in the lever arm domain above the dye, creating a telemark skier configuration in the waiting state between steps (Fig. 1). The exact position of the kink is unknown, although simple geometric arguments indicate the kink is likely between the first and second IQ domains. More generally, our extension of FIONA to enable nanometer tracking of GFP enables monitoring of conformational changes in proteins that are not readily labeled by exogenous dyes.

SUPPLEMENTARY MATERIAL

An online supplement to this article can be found by visiting BJ Online at http://www.biophysj.org. (The supplement shows a diagram of the sample chamber described in the Materials and Methods section.)

We thank Fei Wang for help in the baculovirus expression. We also thank Yale E. Goldman and Ahmet Yildiz for helpful discussions.

This work was supported by the National Institutes of Health (grant AR44420 to P.R.S.).

REFERENCES

Ali, M. Y., S. Uemura, K. Adachi, H. Itoh, K. Kinosita, Jr., and S. Ishiwata. 2002. Myosin V is a left-handed spiral motor on the right-handed actin helix. *Nat. Struct. Biol.* 9:464–467.

Axelrod, D. 1989. Total internal reflection fluorescence microscopy. *Methods Cell Biol.* 30:245–270.

Bartko, A. P., and R. M. Dickson. 1999a. Imaging three-dimensional single molecule orientations. *J. Phys. Chem. B.* 103:11237–11241.

Bartko, A. P., and R. M. Dickson. 1999b. Three-dimensional orientations of polymer-bound single molecules. *J. Phys. Chem. B.* 103:3053–3056.

Burgess, S., M. Walker, F. Wang, J. R. Sellers, H. D. White, P. J. Knight, and J. Trinick. 2002. The prepower stroke conformation of myosin V. *J. Cell Biol.* 159:983–991.

Dominguez, R., Y. Freyzon, K. M. Trybus, and C. Cohen. 1998. Crystal structure of a vertebrate smooth muscle myosin motor domain and its complex with the essential light chain: visualization of the pre-power stroke state. *Cell.* 94:559–571.

Forkey, J. N., M. E. Quinlan, M. Alexander Shaw, J. E. T. Corrie, and Y. E. Goldman. 2003. Three-dimensional structural dynamics of myosin V by single-molecule fluorescence polarization. *Nature.* 422:399–404.

Harada, Y., K. Sakurada, T. Aoki, D. D. Thomas, and T. Yanagida. 1990. Mechanochemical coupling in actomyosin energy transduction studied by in vitro movement assay. *J. Mol. Biol.* 216:49–68.

Howard, J. 1997. Molecular motors: structural adaptations to cellular functions. *Nature.* 389:561–567.

Hua, W., J. Chung, and J. Gelles. 2002. Distinguishing inchworm and hand-over-hand processive kinesin movement by neck rotation measurements. *Science.* 295:844–848.

Kubitscheck, U., O. Kuckmann, T. Kues, and R. Peters. 2000. Imaging and tracking of single GFP molecules in solution. *Biophys. J.* 78:2170–2179.

Mehta, A. 2001. Myosin learns to walk. *J. Cell Sci.* 114:1981–1998.

Mehta, A. D., R. S. Rock, M. Rief, J. A. Spudich, M. S. Mooseker, and R. E. Cheney. 1999. Myosin-V is a processive actin-based motor. *Nature.* 400:590–593.

Peterman, E. J. G., S. Brasselet, and W. E. Moerner. 1999. The fluorescence dynamics of single molecules of green fluorescent protein. *J. Phys. Chem. A.* 103:10553–10560.

Pierce, D. W., N. Hom-Booher, and R. D. Vale. 1997. Imaging individual green fluorescent proteins. *Nature.* 388:338.

Purcell, T. J., C. Morris, J. A. Spudich, and H. L. Sweeney. 2002. Role of the lever arm in the processive stepping of myosin V. *Proc. Natl. Acad. Sci. USA.* 99:14159–14164.

Rief, M., R. S. Rock, A. D. Mehta, M. S. Mooseker, R. E. Cheney, and J. A. Spudich. 2000. Myosin-V stepping kinetics: a molecular model for processivity. *Proc. Natl. Acad. Sci. USA.* 97:9482–9486.

Rock, R. S., S. E. Rice, A. L. Wells, T. J. Purcell, J. A. Spudich, and H. L. Sweeney. 2001. Myosin VI is a processive motor with a large step size. *Proc. Natl. Acad. Sci. USA.* 98:13655–13659.

Rosenfeld, S. S., P. M. Fordyce, G. M. Jefferson, P. H. King, and S. M. Block. 2003. Stepping and stretching. How kinesin uses internal strain to walk processively. *J. Biol. Chem.* 278:18550–18556.

Sakamoto, T., F. Wang, S. Schmitz, Y. Xu, Q. Xu, J. E. Molloy, C. Veigel, and J. R. Sellers. 2003. Neck length and processivity of myosin V. *J. Biol. Chem.* 278:29201–29207.

Schmidt, T., G. J. Schutz, W. Baumgartner, H. J. Gruber, and H. Schindler. 1996. Imaging of single molecule diffusion. *Proc. Natl. Acad. Sci. USA.* 93:2926–2929.

Spudich, J. A. 2001. The myosin swinging cross-bridge model. *Nat. Rev. Mol. Cell Biol.* 2:387–392.

Swaminathan, R., C. P. Hoang, and A. S. Verkman. 1997. Photobleaching recovery and anisotropy decay of green fluorescent protein GFP-S65T in solution and cells: cytoplasmic viscosity probed by green fluorescent protein translational and rotational diffusion. *Biophys. J.* 72:1900–1907.

Thompson, R. E., D. R. Larson, and W. W. Webb. 2002. Precise nanometer localization analysis for individual fluorescent probes. *Biophys. J.* 82: 2775–2783.

Tokunaga, M., K. Kitamura, K. Saito, A. H. Iwane, and T. Yanagida. 1997. Single molecule imaging of fluorophores and enzymatic reactions achieved by objective-type total internal reflection fluorescence microscopy. *Biochem. Biophys. Res. Commun.* 235:47–53.

Veigel, C., F. Wang, M. L. Bartoo, J. R. Sellers, and J. E. Molloy. 2002. The gated gait of the processive molecular motor, myosin V. *Nat. Cell Biol.* 4:59–65.

Walker, M. L., S. A. Burgess, J. R. Sellers, F. Wang, J. A. Hammer III, J. Trinick, and P. J. Knight. 2000. Two-headed binding of a processive myosin to F-actin. *Nature.* 405:804–807.

Wang, F., L. Chen, O. Arcucci, E. V. Harvey, B. Bowers, Y. Xu, J. A. Hammer III, and J. R. Sellers. 2000. Effect of ADP and ionic strength on the kinetic and motile properties of recombinant mouse myosin V. *J. Biol. Chem.* 275:4329–4335.

Wu, X., F. Wang, K. Rao, J. R. Sellers, and J. A. Hammer III. 2002. Rab27a is an essential component of melanosome receptor for myosin Va. *Mol. Biol. Cell.* 13:1735–1749.

Yildiz, A., J. N. Forkey, S. A. McKinney, T. Ha, Y. E. Goldman, and P. R. Selvin. 2003. Myosin V walks hand-over-hand: single fluorophore imaging with 1.5-nm localization. *Science.* 300:2061–2065.